PERSPECTIVE • OPEN ACCESS

Neuromorphic principles for machine olfaction

To cite this article: Nik Dennler *et al* 2025 *Neuromorph. Comput. Eng.* **5** 023001

View the article online for updates and enhancements.

You may also like

NEUROMORPHIC
Computing and Engineering

PERSPECTIVE

Neuromorphic principles for machine olfaction

Nik Dennler[1,2,*] ⓘ, Aaron True[3] ⓘ, André van Schaik[1] ⓘ and Michael Schmuker[2,*] ⓘ

1 International Centre for Neuromorphic Systems, Western Sydney University, Kingswood, NSW, Australia
2 Biocomputation Group, Centre for Data Innovation Research, University of Hertfordshire, Hatfield, United Kingdom
3 Department of Civil, Environmental and Architectural Engineering, University of Boulder Colorado, Boulder, CO, United States of America
* Authors to whom any correspondence should be addressed.

E-mail: dennlern@ethz.ch and m.schmuker@biomachinelearning.net

Abstract

Neuromorphic computing, exemplified by breakthroughs in machine vision through concepts like address-event representation and send-on-delta sampling, has revolutionised sensor technology, enabling low-latency and high dynamic range perception with minimal bandwidth. While these advancements are prominent in vision and auditory perception, their potential in machine olfaction remains under-explored, particularly in the context of fast sensing. Here, we outline the perspectives for neuromorphic principles in machine olfaction. Considering the physical characteristics of turbulent odour environments, we argue that event-driven signal processing is optimally suited to the inherent properties of olfactory signals. We highlight the lack of bandwidth limitation due to turbulent dispersal processes, the characteristic temporal and chemical sparsity, as well as the high information density of the odour landscape. Further, we critically review and discuss the literature on neuromorphic olfaction; particularly focusing on neuromorphic principles such as event generation algorithms, information encoding mechanisms, event processing schemes (spiking neural networks), and learning. We discuss that the application of neuromorphic principles may significantly enhance response time and task performance in robotic olfaction, enabling autonomous systems to perform complex tasks in turbulent environments—such as environmental monitoring, odour guided search and rescue operations, and hazard detection.

1. Introduction

The sensory capabilities of animals still surpass the limits of technology in many domains. It is therefore not surprising that the underlying principles have long inspired devices and algorithms for sensing in machines. Neuromorphic computing is a prime example of this approach [1–3]. In machine vision, bio-inspiration and neuromorphic principles have enabled breakthroughs in sensor technology. In particular, the send-on-delta sampling algorithm [4] and the *address-event representation* [5] have enabled low-latency and high dynamic range sensing, requiring little bandwidth to represent sparse signals [6, 7]. Today, the groundbreaking developments in neuromorphic technology have culminated in commercially available products and various applications where event-based vision solves problems that are difficult to tackle with conventional frame-based image sensors [8, 9]. The principle of dynamic sampling has since been extended to other sensing paradigms, most prominently in the research of neuromorphic auditory perception [10].

Olfaction, or the sense of smell, involves complex signal processing and pattern recognition to identify and discriminate between a vast array of chemical compounds [11, 12]. Computational models of olfaction aim to replicate these biological processes, yielding new algorithms [13, 14] and sensor technologies [15, 16] for mimicking the highly efficient and adaptive nature of animal olfactory systems. Here, we explore what opportunities event-driven processing may deliver in machine olfaction.

2. Why neuromorphic olfaction?

To determine whether neuromorphic computing may benefit machine olfaction, we shall examine the conditions under which such mechanisms have proven effective. A compelling argument by Liu *et al* [17] suggests attributing to a signal its degree of bandlimitation. This may indicate the presence of a stable mapping function between the signal and uniformly spaced samples, or alternatively suggest that dynamically acquired samples could be superior in representing the signal. In vision, for instance, natural scenes contain motions at varying velocities, and choosing a constant camera frame rate that matches the fastest observed motion is inefficient [17]. More fundamentally, high-contrast (Dirac- or step-function-like) scenes are not bandlimited in space, while any moving object is not bandlimited in time. Here, nonuniform and data-driven/dynamic sampling may be favourable. Contrary, audio signals (such as speech) are inherently bandlimited by the transmission medium air: Low frequencies (≈ 1 Hz) require massive sources (e.g. earthquakes), while high frequencies (ultrasound, >20 kHz) attenuate rapidly [18]. Thus, irrespective of the recording device, an upper and lower limit of a signal's bandwidth may be determined in advance, therefore allowing the selection of a periodic sampling rate that captures the relevant signal with minimal aliasing.

Temporal and spatial sparsity of signals also suggest event-based processing [19, 20]. When imaging natural scenes, most regions do not change significantly over short periods of time (temporal sparsity) and contain large areas of similar intensity or colour (spatial sparsity). Both biological and neuromorphic vision systems tend to encode information efficiently by emphasising changes and discontinuities rather than uniform areas, which is aligned with the efficient coding hypothesis [21, 22]. Thus, signal sparsity aids in explaining the effectiveness of event-based processing for visual stimuli, and may indicate applicable regimes for other sensing modalities [23].

What is the situation in olfaction?
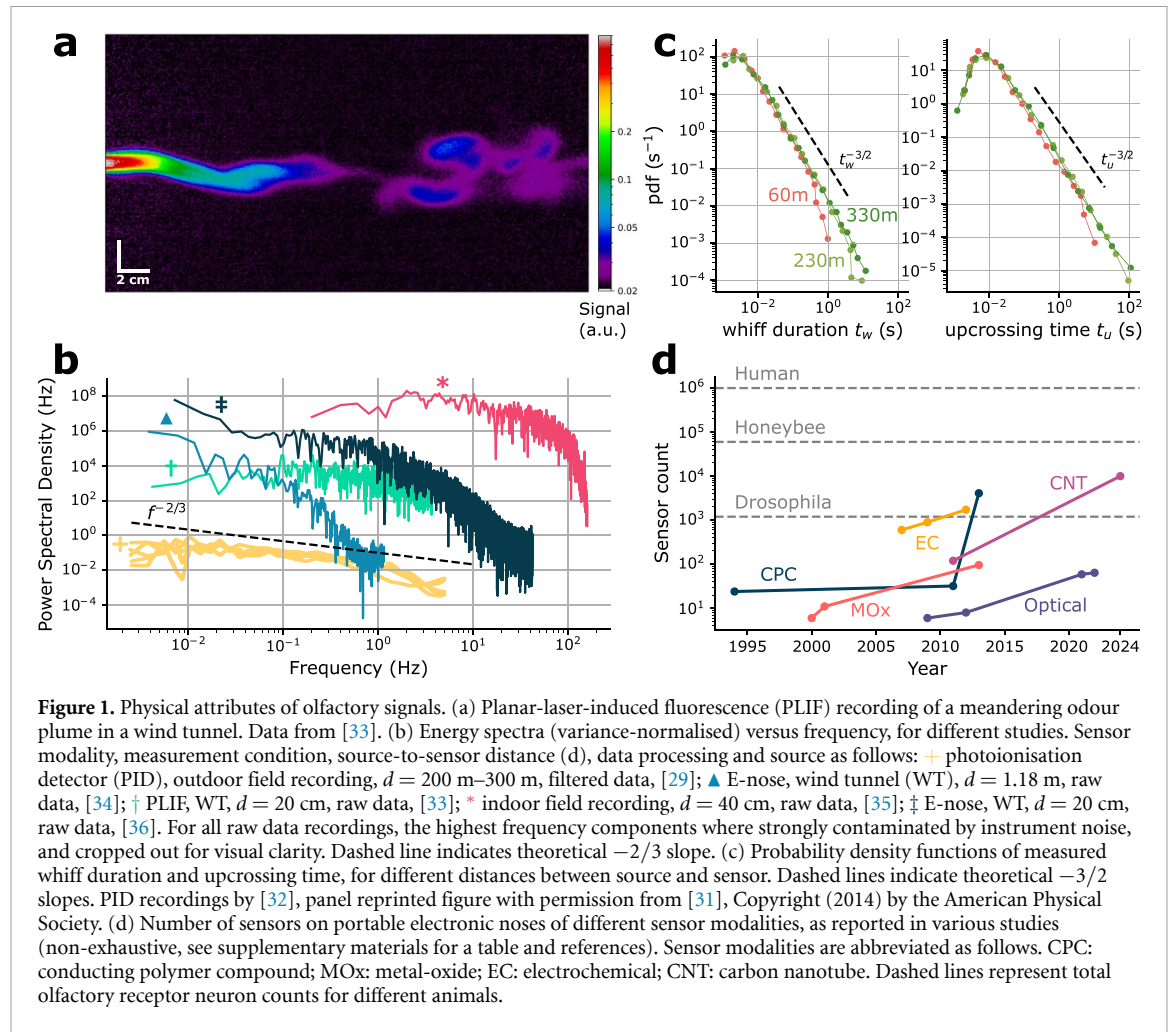
2.1. Olfaction is not bandlimited

Under virtually all relevant natural conditions, odorants are transported by turbulent dispersal. This process is fundamentally different from smooth and laminar transport, as it creates highly dynamic and unpredictable concentration fields. Turbulent flows are characterised by eddies, i.e. vortices of variable size. Large eddies dissipate their power into smaller eddies [24, 25], cascading down to the molecular level, where energy is dissipated into heat through friction [26]. This process creates odour structures spanning a range of length scales, producing characteristic temporal odour fluctuations as they are transported across a sensor.

The statistics of these odour fluctuations depend on (a) environmental flow conditions, and (b) the odour source configuration. Environmental flow conditions set the relative importance of the physical processes acting on odour structures en route to the sensor. This includes fluid dynamic strain, which locally enhances concentration gradients, and molecular diffusion, which diminishes them. The source configuration includes factors like its dimensions, mass flow rate, buoyancy, and proximity to boundaries. Collectively, these factors produce variance in the odour concentration field, where the size L of an odour plume relative to the eddies predicts what fluid dynamic processes drive local concentration fluctuations [27]. If eddies are larger than L—which is often the case very close to the odour source—they contribute mostly to plume meandering, i.e. the irregular motion of the fluid volume's centre of mass (see figure 1(a)). Conversely, if eddies are smaller than L—as encountered at a greater distance from the source—they contribute to turbulent diffusion characterised by shearing, distortion, and expansion of the plume.

The odour concentration fluctuations in turbulent plumes are distributed as a power law [28, 29] and span several orders of magnitude. In particular, it has been postulated and empirically shown [29] that for fully developed turbulence regimes (i.e. far away from the source, where the Reynolds number Re is high), the frequency energy spectrum $nS(n)$ exhibits a log–log relationship with the frequency n as

$$ nS(n) = a\epsilon^{2/3} \left(\frac{n}{U} \right)^{-2/3}, \tag{1} $$

where a and ϵ are a universal constant and the rate of turbulent energy dissipation respectively, and U is the mean wind speed. This implies that for fluctuations in odour concentration, there is a non-vanishing energy contribution even at very high frequencies. Figure 1(b) displays a collection of power spectral densities, calculated from data of various studies. All the considered datasets exhibit a pronounced log–log power law—collectively covering frequencies that span five orders of magnitude—however, variations in turbulence regime, sensor modality, and post-processing methods may cause deviations from the theoretical $f^{-2/3}$ slope. Therefore, unlike other sensory modalities such as auditory perception, signals derived from the odour space are not subject to narrow bandwidth limitations.

Figure 1. Physical attributes of olfactory signals. (a) Planar-laser-induced fluorescence (PLIF) recording of a meandering odour plume in a wind tunnel. Data from [33]. (b) Energy spectra (variance-normalised) versus frequency, for different studies. Sensor modality, measurement condition, source-to-sensor distance (d), data processing and source as follows: + photoionisation detector (PID), outdoor field recording, d = 200 m–300 m, filtered data, [29]; ▲ E-nose, wind tunnel (WT), d = 1.18 m, raw data, [34]; † PLIF, WT, d = 20 cm, raw data, [33]; * indoor field recording, d = 40 cm, raw data, [35]; ‡ E-nose, WT, d = 20 cm, raw data, [36]. For all raw data recordings, the highest frequency components where strongly contaminated by instrument noise, and cropped out for visual clarity. Dashed line indicates theoretical $-2/3$ slope. (c) Probability density functions of measured whiff duration and upcrossing time, for different distances between source and sensor. Dashed lines indicate theoretical $-3/2$ slopes. PID recordings by [32], panel reprinted figure with permission from [31], Copyright (2014) by the American Physical Society. (d) Number of sensors on portable electronic noses of different sensor modalities, as reported in various studies (non-exhaustive, see supplementary materials for a table and references). Sensor modalities are abbreviated as follows. CPC: conducting polymer compound; MOx: metal-oxide; EC: electrochemical; CNT: carbon nanotube. Dashed lines represent total olfactory receptor neuron counts for different animals.

2.2. Olfaction is temporally sparse

Intermittency is a defining feature of turbulent odour plumes [30, 31]. Single odour packets (also 'whiffs' or 'bouts') or clusters of odour packets (also 'clumps') are separated by periods of no signal (also 'blanks'). The timescales of bout durations and inter-bout intervals, as well as bout amplitude (or odour concentration) and bout-per-clump counts, depend on environmental flow conditions—most notably the structure of the mean and fluctuating velocity fields—and the vector between the encounter point and odour source. Relevant statistical characterisations of whiffs, clumps, and blanks have been postulated and tested [31]. In particular, both the duration of a whiff t_w (the time between the concentration signal crossing a threshold c_thr upwards and downwards) and the upcrossing duration t_u (the time between the upward crossings corresponding to two whiffs) are distributed according to power laws:

$$p\left(t_w\right) = \frac{1}{\tau}\left(\frac{t_\mathrm{w}}{\tau}\right)^{-3/2} g_\mathrm{w}\left(t_\mathrm{w}\right), \qquad\qquad p\left(t_\mathrm{u}\right) = \frac{1}{\tau}\left(\frac{t_\mathrm{u}}{\tau}\right)^{-3/2} g_\mathrm{u}\left(t_\mathrm{u}\right). \qquad (2)$$

The functions g_w and g_u describe cut-offs that are exponential for large arguments, while τ is a diffusion time constant. Figure 1(c) displays field recordings of turbulent odours [32], demonstrating the $t_x^{-3/2}$ power law, spanning four orders of magnitude for both whiff duration and upcrossing times. While short odour packages at milliseconds or less [31] are possible and most likely, the probability for extended periods of no incoming odour packages is non-vanishing. In such terms, olfactory signals are sparse in time.

2.3. The odour space is informative, tangible, and suggesting event-driven sensing

Intuitively, the notion of turbulence may suggest elusiveness, disorder or even chaos. However, the statistics of odour encounters in turbulent environments encode spatial information of the odour source and its surroundings. In particular, measured bout concentration variations as well as intermittency are indicators of the plume dimensions [37]. The degree of temporal correlation between two encountered odours at a single point can indicate their separating distance [38]. Conversely, analysing the correlation between same-odour encounters at multiple points in space indicates the relative position of the source [39].

Additionally, several plume features have been shown to reproducibly vary with distance and direction between the sensor and odour source, such as the concentration amplitude and first derivative of a bout [40], the degree of intermittency [41], and the average bout count [42].

While olfaction is temporally sparse, it is not subject to bandlimitations, suggesting that many plume features can be captured reliably only if the plume is sensed and processed fast enough. In fact, stationary measurements of odour concentration fluctuations occur at frequencies exceeding 100 Hz [43], while individual odour encounters can last few milliseconds or less [31]. Many animals exhibit remarkable abilities in rapidly detecting and processing short odour stimuli. For instance, insects olfactory receptor neurons' (ORNs) response latency is less than 2 ms [44, 45], and odour stimuli fluctuations can be resolved at frequencies of over 100 Hz [44]. This enables them to efficiently track dynamics of fast odour signals [46], eventually leading to solving complex tasks such as odour source localisation in turbulent environments [47, 48], or perceptually segregate mixed odours from different sources [35, 38, 48]. In machine olfaction, the relatively slow sensor response and recovery times of electronic nose devices have been prohibitive for many applications. However, recent advances in sensors and processing algorithms have brought their temporal capabilities closer those of animals. For instance, we reported on a miniaturised electronic nose with an odour response time in the millisecond regime [36], outperforming mice in their temporal capabilities on equivalent tasks.

The observed power law in odour concentration extends to small spatial scales, which in turn correspond to very high frequencies. Accurately extracting information requires high temporal resolution, yet efficiency considerations must account for the signals' sparsity in time and sensor activation. We argue that event-driven processing schemes are optimal in this regime. They allow for efficiently handling the observed scale-invariance and heavy-tailed distributions of odour encounters, as they inherently represent information with high temporal precision and the least possible temporal quantisation, while achieving minimal activity in the frequent periods where no odour is present. For instance, a neuromorphic sensor could generate events in response to the onset and offset of odour whiffs, accurately capturing its concentration and duration. During periods of no signal, the system could remain inactive, conserving energy and focusing computational resources on the next significant event.

2.4. Olfaction is chemically sparse, motivating activation-driven and adaptive sensing

Chemical space is vast. It has been estimated that the number of theoretically synthesisable drug-like molecules, i.e. that obey certain rules regarding oral bioavailability, approaches 10^{60} [49, 50]. Projects like GDB [51] aim at enumerating as much as possible of this space, currently containing close to 165 billion small molecules. The subset of molecules perceived as odorous is suggested to count around 40 billion [52]. To successfully navigate and interact with this vast chemical space, evolution has equipped the animal kingdom with a large number of ORNs. For instance, fruit flies (*Drosophila*) express around 1500 ORNs of 60 different types [53], while honeybees have around 60 000 ORNs of 160 different types [54]. Those numbers pale in comparison to mammals; humans have around a million ORNs of 300 types [55] (postulated to be aligned to key food odourants [56]), while certain dogs have up to 300 million ORNs [57].

At high odour concentrations, i.e. parts-per-million (*ppm*) or higher, the odour representation at the receptor and glomerular levels is typically combinatorial, relying on broad tuning of the receptors [58–64]. However, naturally occurring odourant levels rarely exceed the parts-per-billion (*ppb*) range, calling for a more nuanced treatment of this regime [65]. In fact, recent evidence indicates that at these bio-relevant concentrations (*ppb* and lower), mammalian olfactory sensory neurons exhibit sparse activation, with some responding selectively to a single odourant [66–68]. Further downstream from the sensory neurons, both mammals and insects exhibit high degrees of sparsity. In the insect olfactory system, the sparse representation of odours in the mushroom body [69] is maintained via a normalising negative-feedback loop over a wide range of input conditions [70]. Similarly, the mitral cells of the mammalian olfactory bulb (OB) respond sparsely to glomeruli inputs [71], which emerges from the excitatory-inhibition balance between mitral cells and granule cells [72]. While the capacity to distinguish millions of odours likely depends on broad receptor activation at high concentrations, such scenarios may be ecologically rare. In natural settings, animals may only need to detect and discriminate a small subset of behaviourally relevant odourants, such as those associated with food, mates, or predators. Indeed, Dunkel *et al* [56] proposed that mammalian olfactory perception is structured around a limited number of key food odourants, suggesting that sparsity at low concentrations may reflect an evolutionary optimisation towards ecological relevance rather than a limitation in olfactory coding capacity.

In machine olfaction, the term 'electronic nose' refers to an array of individually addressable gas or odour sensors. The activation across sensors is often interpreted as a combinatorial code, or odour fingerprint, which ideally correlates with odour identity and concentration [73]. Different sensing elements are used, such as electrochemical sensors, conducting polymer compound gas sensors, Metal-Oxide (MOx) gas

sensors, optical gas sensors, and carbon-nanotube gas sensors. They vary in their capabilities (e.g. sensitivity and response time) and constraints (e.g. power consumption, form factor, and sensor drift), and are typically selected according to their use cases. In theory, a larger set of sensors with slightly different chemical selectivity would improve the capability of an electronic nose device to discriminate different odorants and mixtures. In line with this postulate, the reported numbers of individual sensing elements embedded on electronic nose devices have been growing steadily (see figure 1(d)), most recently surpassing 10 000 sensors [74].

Analogous to biological olfaction, it has been demonstrated that the activation across large sensor arrays is non-uniform, and that it often sufficient to consider a sparse subset of the available sensing elements [74, 75]. In fact, the duality between sparse and broad activation observed in biological systems may be a desirable feature in artificial olfaction as well. At low concentrations, high specificity is advantageous for detecting trace compounds in industrial or safety-critical contexts—such as the selective detection of benzene [76] or methanol [77]. Conversely, broader sensor activation at higher concentrations could enhance robustness and generalisation when encountering unfamiliar odourants in complex or uncontrolled environments, much like the adaptability seen in natural olfaction. Neuromorphic implementations of electronic noses could thus benefit from incorporating dynamic tuning mechanisms that reflect this biologically inspired balance between selectivity and coverage. This could again motivate event-based sensor processing: Efficiency increases could be achieved by sampling and processing data from the growing number of sensors activation-driven, adaptive, and in parallel; which neuromorphic algorithms and substrates inherently support [1, 2].

3. Neuromorphic odour sampling and signal processing

In neuromorphic vision, a vast majority of studies and applications are based on events that are generated by adaptive threshold crossing (send-on-delta) of a logarithmically scaled brightness signal, and represented via their pixel address x and time t. Most prominently, the dynamic vision sensor [6] integrates this in a circuit, and produces events e_k of the shape

$$e_k\left(\boldsymbol{x_k}, t_k, p_k\right), \tag{3}$$

where p_k represents the polarity of change, i.e. $p \in [-1, 1]$. For processing, the events are then either represented as an accumulated image frame, or via particular encoding schemes such as time surfaces or voxel grids [8], or as individual events to be directly processed via spiking neural networks (SNN). Yet, there exists a multitude of other methods for generating, representing and processing events.

In the following, we introduce, review, and critically discuss different principles regarding event-based sampling and signal processing for neuromorphic olfaction.

3.1. Event generation and information encoding
3.1.1. Biological action potentials (AP)
In biological olfaction, similar principles across phyla are observed to generate odour response spikes at the olfactory receptor level. Insects embed ORN in hair-like structures on their antennae, while in mammals ORNs are located in the olfactory epithelium that covers internal parts of the nasal cavity [78]. In both cases, once an odour molecule has bound to its corresponding receptor [79], a signal transduction cascade is initiated, leading to the opening of ion channels that ultimately cause the neuron to depolarise and initiate an AP. The AP, which can be understood as a binary event, is transmitted to and further processed in the insect antennal lobe (OB) and mammalian OB, respectively.

3.1.2. Artificial neurons and current injection
Various methods for converting a continuous gas sensor response into binary events have been introduced. One approach (see figure 2(a)) involves simulating or emulating the membrane potential V_{m} of an artificial spiking neuron, and feeding the sensor response as an input current $I(t)$:

$$\frac{\mathrm{d}V_{\mathrm{m}}\left(t\right)}{\mathrm{d}t} = -\frac{V_{\mathrm{m}}\left(t\right) - V_{\mathrm{rest}}}{R_{\mathrm{m}}C_{\mathrm{m}}} + \frac{I(t)}{C_{\mathrm{m}}}. \tag{4}$$

Here, R_{m}, C_{m} and V_{rest} are the membrane's resistance, capacitance, and resting potential, respectively. An event is generated whenever V_{m} crosses a fixed threshold, followed by resetting V_{m} to its resting potential. Both early and more recent studies in neuromorphic olfaction have leveraged this approach extensively [80–89] using different neuron models, parameters, and signal conditioning methods. The method is particularly applicable for hardware SNN implementations, as the computing substrate itself can be used to

generate the spikes. Conversely, the approach is less suitable for FPGA and digital implementations, as the simulation of differential equations is computationally expensive. Similarly, events can be generated via a biased Poisson process [90]. This has been utilised to emulate ORN excitations [91] in neuromorphic olfactory models; however, it could also be used to generate odour response events by biasing the Poisson process towards an average event rate that is proportional to the odour-specific sensor response. All those approaches represent a form of rate code, i.e. the event rate being proportional to the sensor response [92], or—in the case of multiple sensors—a population code. While offering a noise-resilient and robust encoding, information transmission relies on downstream event integration and tends to be slow.

3.1.3. Latency-representation events
Other information encoding schemes rely on the precise timing of events. For instance, single events may be generated at latencies Δt_{ij} that are proportional to the log-response of sensor j to an odour i, i.e. $\Delta t_{ij} \propto \ln S_j(t)$, which allows considering the relative latency (i.e. the rank) of the different sensors as a concentration-independent odour mapping [93–96]. Similar methods that use transient features instead of the raw signal have been proposed [97, 98]. Albeit being potentially fast and highly sparse, this encoding breaks down at single noise events, and in the reported form is not suited for dynamically changing signals due to the lack of a reset signal. Similar, yet more sophisticated methods have been proposed, where transient features are converted into events of different latencies [99, 100], to be further processed by an SNN.

3.1.4. Change detection events
Another approach—as prominently featured in event-based vision—is using the send-on-delta algorithm [4] to generate events that correspond to positive or negative changes in the sensor response [101–104]. In particular, if the signal crosses a reference voltage plus or minus a set threshold, a positive or negative change event is generated and the reference voltage shifted up- or downwards by the threshold (see figure 2(a)). In vision, the signal is typically preconditioned through logarithmic scaling, which increases the dynamical range drastically [6]. In olfaction, however, this may not be necessary, as the transfer function of many gas sensors implicitly scales the encountered odour concentration range [105].

The send-on-delta method is fast, sparse, and robust; yet as it tracks changes only, it does not provide the absolute signal intensity. In vision, intensity information is often not needed, however is retained in the Asynchronous Time-based Image Sensor (ATIS) pixel design [7]. Besides generating positive and negative change detection events, the mechanism employs an extra channel containing pairs of events, with a time difference inversely proportional to the absolute signal intensity (see figure 2(a)). This concept loosely resembles the dual-pathway observed in the mammalian OB [106], which has inspired a series of studies adapting the ATIS circuit for mixed-signal event-based gas concentration measurements [107–109]. A sparser and more straightforward event representation is achieved by providing separate event channels for fixed amplitude levels, as demonstrated first for an event-based speech processing audio front end [110]. Whenever an amplitude level is crossed upwards or downwards, an event in the corresponding channel is generated (see figure 2(a)). This method may be particularly effective whenever the amplitude range of the signal is known beforehand, which is often the case for gas sensors.
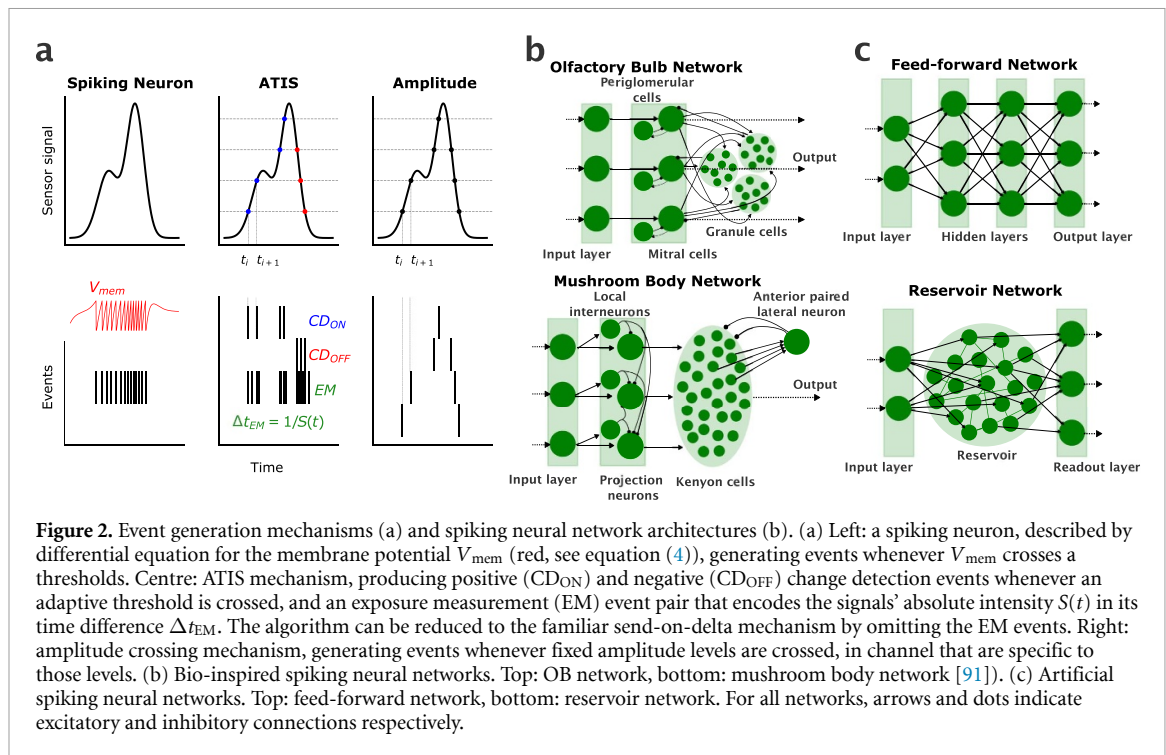
3.1.5. Events encoding turbulent plume features
The intermittent nature of turbulent odour plumes may suggest encoding temporal features of the plume, such as bouts and blanks, in the event trains. Recent evidence from neuroscience indicates that animals apply similar principles. For instance, large-scale temporal odour features—specifically plume onset, plume offset, and whiff encounter—are encoded in the mammalian OB spike output, both at the single-cell and population levels [111]. These features are critical for odour-guided navigation [112, 113] and source localisation tasks [114]. Such an approach has been demonstrated by isolating the bout onset from the sensor response through Kalman filtering, and subsequently generating change events through send-on-delta sampling [115]. In a stereo sensing setup, this method allowed for estimating bout velocity by considering the relative event latencies between sensors [115]. Other methods that approximate the plume dynamics from the sensor response, such as cascaded filtering [42] or blind deconvolution [116], could be combined with send-on-delta or ATIS mechanisms for generating informative and task-relevant event patterns.

3.2. Event-based signal processing and learning
3.2.1. Biological neural networks
Evolution provides us with effective mechanisms for processing event trains generated by thousands to millions of ORN) ORNs that express the same type of OR converge onto spatially separated structures called glomeruli, which are found in both the mammalian OB and the insect AL. Interneurons, such as the mammalian granule cells and periglomerular cells, modulate glomerular activity through inhibitory and

Figure 2. Event generation mechanisms (a) and spiking neural network architectures (b). (a) Left: a spiking neuron, described by differential equation for the membrane potential V_{mem} (red, see equation (4)), generating events whenever V_{mem} crosses a thresholds. Centre: ATIS mechanism, producing positive (CD_{ON}) and negative (CD_{OFF}) change detection events whenever an adaptive threshold is crossed, and an exposure measurement (EM) event pair that encodes the signals' absolute intensity $S(t)$ in its time difference Δt_{EM}. The algorithm can be reduced to the familiar send-on-delta mechanism by omitting the EM events. Right: amplitude crossing mechanism, generating events whenever fixed amplitude levels are crossed, in channel that are specific to those levels. (b) Bio-inspired spiking neural networks. Top: OB network, bottom: mushroom body network [91]). (c) Artificial spiking neural networks. Top: feed-forward network, bottom: reservoir network. For all networks, arrows and dots indicate excitatory and inhibitory connections respectively.

excitatory interactions, which enhances odour separability and noise resilience. Projection neurons, such as mitral cells, relay the glomerular activity to higher brain centres, which includes the olfactory cortex in mammals, and the mushroom bodies and lateral horns in insects [78].

3.2.2. SNNs

In artificial olfaction, besides directly considering one of the discussed encoding schemes, such as the average event rate or the order (rank) of incoming events, the typical approach to processing asynchronous events is using SNNs. SNNs represent a class of artificial neural networks that mimic biological neural systems more closely than traditional neural networks (ANNs, such as the multilayer perceptrons), by implementing a network of artificial spiking neurons as described by equation (4). The key difference to ANNs is that SNNs typically incorporate the precise timing of events in their operation, and activate subsequent nodes only when a fixed activation threshold is crossed, allowing for asynchronous and data-driven computing [117]. SNNs build the foundation for (non-von-Neumann) neuromorphic computers, which are characterised by their highly parallel operation and collocated processing and memory units [2].

3.2.3. Bio-inspired SNNs

Various studies have focused on implementing concepts from biological olfaction systems, either in simulation or hardware. Many of these studies concentrate on the mammalian OB and glomeruli models, which perform a form of dimensionality reduction through excitatory and inhibitory dynamics (see figure 2(b), top for a circuit diagram). Early works implemented OB models on very-large-scale-integration (VLSI) hardware and trained them either via Hebbian learning [80] or Spike-Timing-Dependent Plasticity (STDP) [81, 82], or self-organizing models [118]. The STDP approach has since been integrated into low-power electronic nose systems [83, 100], demonstrating effectiveness in tackling sensor drift [119]. A noteworthy SNN implementation of an STDP-based glomerulus model that couples its activity with gamma oscillation promises to perform noise-robust learning from single data instances [120]; however, the reported evaluation protocols are not conclusive [121]. Recent efforts focus on few-shot class-incremental learning [98] or on fusing the OB network with an SNN that is driven by visual stimuli [122].

Other biology-inspired studies choose to implement parts of the insect AL [123] (see figure 2(b), bottom for a circuit diagram). Early works implemented simplified AL models on VLSI hardware [124] and on neuromorphic computing substrates [125], which have been extended to more complex models that focus on excitatory-inhibitory dynamics [91]. Further studies implemented AL models and included learning via STDP [101, 126, 127], supervised soft-winner-take-all mechanisms [84, 128], and combinations of unsupervised self-organisation processes and supervised synaptic plasticity rules [85]. A noteworthy contribution has been made by further abstracting the biological networks; implementing a two-layer SNN

that performs concentration-invariant odour detection through event synchrony [89]. In addition to sensory processing and learning, multiple studies have demonstrated that motor control behaviour may be implemented by the insect mushroom body circuitry [129–131], therefore allowing to close the sensory-motor loop in neuromorphic systems [132].

3.2.4. Feed-forward SNNs

Feed-forward SNNs are more commonly used for neuromorphic vision or auditory perception, as they can simplify model implementation and training procedures by transmitting information in just one direction, i.e. with no recurrent connections. See figure 2(c), top for an illustration of the concept. In neuromorphic olfaction, similar approaches have been demonstrated. For instance, a two-layer SNN was implemented and trained via STDP on a neuromorphic chip [102], and then used to differentiate between roasted malt samples [104]. Further, a four-layer SNN was trained from input neuron activation (offline, via backpropagation), then demonstrated to be of practical use on a food science task [87]. While feed-forward SNNs offer simple training, they do not support the recurrent dynamics observed in biological olfactory circuits and hence might be limited in their ability to efficiently deal with olfactory signals.

3.2.5. Reservoir SNNs

A reservoir network, or liquid state machine, is a computing concept that can be implemented using SNNs: An input layer projects onto a reservoir of neurons, typically consisting of sparse, recurrent, and excitatory-inhibitory interconnections using randomised and untrained weights. A readout layer connects to a subset of these neurons, with weights that are trained via supervised learning. See figure 2(c), bottom for an illustration. This method allows for casting the input to a spatially and temporally higher-dimensional space [2, 133]. In fact, the projection into a high-dimensional space inherent to the insect mushroom body [134] can be modelled using reservoir networks, which may be leveraged when designing neuromorphic circuits [127]. Further, the concept has inspired reservoir SNNs with cubic network connectivity used for event-based odour data classification [99, 135], as well as implementations based on memristive devices [136]. A recent review argues that reservoir computing is particularly well suited to match the physics in photoelectrochemical devices [137], which may make it an intriguing candidate for emerging optical odour sensing technologies [75].

4. Discussion

Based on the physical characteristics of turbulent odour environments, we reason that neuromorphic computing is highly beneficial for machine olfaction. Odour signals span a space of billions of different odourants and are presented to detectors as fluctuations following power law distributions across multiple orders of magnitude. Event-driven processing schemes offer an optimal solution by capturing salient features at high temporal precision, while energy consumption and data bandwidth can be preserved during idle periods or for inactive sensor nodes. This approach aligns well with biological systems' efficiency in handling sparse and dynamic signals.

The key benefit of event-driven processing is the viability of exceptionally high temporal resolution while retaining low data bandwidth; however, none of the reviewed studies in neuromorphic olfaction have emphasised speed. This comes as little surprise, as machine olfaction has only recently seen timescales that approach the capabilities of animals [36]. Nevertheless, the neuromorphic methods for asynchronous sampling and processing presented here are relevant, and could be adapted with little effort to state-of-the-art odour and gas sensors. In particular, the change-detection method and its variants may provide suitable candidates for producing efficient encoding of rapidly changing sensor dynamics. Alternatively, events that explicitly encode temporal features of odour plumes may achieve high information density, as the encoding would be tailored to the underlying physical processes. For processing the generated events, asynchronously driven SNNs can be used. Networks with some degrees of recurrency, such as SNN implementations of the AL or the OB, or the more abstract reservoir SNN, may be particularly well suited for high-speed processing.

Neuromorphic olfaction holds promise for tackling many real-world challenges that require rapid and efficient odour sensing. A set of particularly promising applications are found in olfactory robotics [138], where unmanned ground or aerial vehicles (UGV / UAV) perform odour source localisation and navigation tasks [139, 140]. Examples of such are the use of smoke-sensing drones for wildfire monitoring [141], swarm-based gas source localisation in indoor environments [142], as well as distributed gas discrimination and mapping in emergency response scenarios [143]. Those tasks rely heavily on sensing the environment rapidly and efficiently, under restrictive constraints for form factor and power budget. Equipping robots with neuromorphic olfactory sensing and processing capabilities may lead to significant improvements in

response time and task performance metrics, enabling operation in complex and turbulent environments, as well as allowing for highly optimised power management strategies.

Data availability statement

No new data were created or analysed in this study.

Acknowledgments

Conflict of interest

The authors declare that the research was conducted in the absence of any commercial or financial relationships that could be construed as a potential conflict of interest.

Funding

ORCID iDs

Nik Dennler ⬤ https://orcid.org/0000-0002-0380-2450
Aaron True ⬤ https://orcid.org/0000-0001-9956-5105
André van Schaik ⬤ https://orcid.org/0000-0001-6140-017X
Michael Schmuker ⬤ https://orcid.org/0000-0001-7436-9992

References

[1] Indiveri G *et al* 2011 Neuromorphic silicon neuron circuits *Front. Neurosci.* **5** 1–23
[2] Schuman C D, Kulkarni S R, Parsa M, Mitchell J P, Date P and Kay B 2022 Opportunities for neuromorphic computing algorithms and applications *Nat. Comput. Sci.* **2** 10–19
[3] Christensen D V *et al* 2022 2022 roadmap on neuromorphic computing and engineering *Neuromorph. Comput. Eng.* **2** 022501
[4] Miskowicz M 2006 Send-on-delta concept: an event-based data reporting strategy *Sensors* **6** 49–63
[5] Boahen K 2000 Point-to-point connectivity between neuromorphic chips using address events *IEEE Trans. Circuits Syst. II* **47** 416–34
[6] Lichtsteiner P, Posch C and Delbruck T 2008 A 128 × 128 120 dB 15 microsecond latency asynchronous temporal contrast vision sensor *IEEE J. Solid-State Circuits* **43** 566–76
[7] Posch C, Matolin D and Wohlgenannt R 2011 A QVGA 143 dB dynamic range frame-free PWM image sensor with lossless pixel-level video compression and time-domain CDS *IEEE J. Solid-State Circuits* **46** 259–75
[8] Gallego G *et al* 2020 Event-based vision: a survey *IEEE Trans. Pattern Anal. Mach. Intell.* **44** 154–80
[9] Gehrig D and Scaramuzza D 2024 Low-latency automotive vision with event cameras *Nature* **629** 1034–40
[10] Liu S, Van Schaik A, Mincti B A and Delbruck T 2010 Event-based 64-channel binaural silicon cochlea with Q enhancement mechanisms *Proc. 2010 IEEE Int. Symp. on Circuits and Systems* (IEEE) pp 2027–30
[11] Laurent G, Stopfer M, Friedrich R W, Rabinovich M I, Volkovskii A and Abarbanel H D 2001 Odor encoding as an active, dynamical process: experiments, computation and theory *Annu. Rev. Neurosci.* **24** 263–97
[12] Cleland T A and Linster C 2005 Computation in the olfactory system *Chem. Senses* **30** 801–13
[13] Hopfield J J 1999 Odor space and olfactory processing: collective algorithms and neural implementation *Proc. Natl Acad. Sci.* **96** 12506–11
[14] Dasgupta S, Stevens C F and Navlakha S 2017 A neural algorithm for a fundamental computing problem *Science* **358** 793–6
[15] Gutiérrez J and Horrillo M 2014 Advances in artificial olfaction: sensors and applications *Talanta* **124** 95–105
[16] Larisika M *et al* 2015 Electronic olfactory sensor based on *A. mellifera* odorant-binding protein 14 on a reduced graphene oxide field-effect transistor *Angew. Chem., Int. Ed.* **54** 13245–8
[17] Liu S, Rueckauer B, Anumula J, Huber A, Neil D and Delbruck T 2019 Event-driven sensing for efficient perception *IEEE Signal Process. Mag.* **36** 29–37
[18] Vladišauskas A and Jakevičius L 2004 Absorption of ultrasonic waves in air *Ultragarsas* **50** 46–49
[19] Olshausen B and Field D 2004 Sparse coding of sensory inputs *Curr. Opin. Neurobiol.* **14** 481–7
[20] Delbruck T, Linares-Barranco B, Culurciello E and Posch C 2010 Activity-driven, event-based vision sensors *Proc. 2010 IEEE Int. Symp. on Circuits and Systems* (IEEE) pp 2426–9
[21] Barlow H B 1961 Possible principles underlying the transformations of sensory messages *Sensory Communication* (MIT Press) pp 216–34
[22] Simoncelli E P and Olshausen B A 2001 Natural image statistics and neural representation *Annu. Rev. Neurosci.* **24** 1193–216

[23] Maass W 2015 To spike or not to spike: that is the question *Proc. IEEE* **103** 2219–24

[24] Kolmogorov A N 1941 The local structure of turbulence in incompressible viscous fluid for very large reynolds numbers *Dokl. Akad. Nauk SSSR* **30** 301

[25] Obukhov A 1941 Spectral energy distribution in a turbulent flow *Izv. Akad. Nauk. SSSR. Ser. Geogr. I. Geofiz* **5** 453–66

[26] Orszag S 1973 Statistical theory of turbulence *Fluid Dynamics* (Gordon and Breach) pp 237–374

[27] Cassiani M, Bertagni M B, Marro M and Salizzoni P 2020 Concentration fluctuations from localized atmospheric releases *Bound.-Layer Meteorol.* **177** 461–510

[28] Hanna S R and Insley E M 1989 Time series analyses of concentration and wind fluctuations *Bound.-Layer Meteorol.* **47** 131–47

[29] Mylne K R and Mason P J 1991 Concentration fluctuation measurements in a dispersing plume at a range of up to 1000 m *Q. J. R. Meteorol. Soc.* **117** 177–206

[30] Murlis J, Elkinton J S and Cardé R T 1992 Odor plumes and how insects use them *Annu. Rev. Entomol.* **37** 505–32

[31] Celani A, Villermaux E and Vergassola M 2014 Odor landscapes in turbulent environments *Phys. Rev. X* **4** 041015

[32] Yee E, Chan R, Kosteniuk P R, Chandler G M, Biltoft C A and Bowers J F 1995 Measurements of level-crossing statistics of concentration fluctuations in plumes dispersing in the atmospheric surface layer *Bound.-Layer Meteorol.* **73** 53–90

[33] Connor E G, McHugh M K and Crimaldi J P 2018 Quantification of airborne odor plumes using planar laser-induced fluorescence *Exp. Fluids* **59** 137

[34] Vergara A, Fonollosa J, Mahiques J, Trincavelli M, Rulkov N and Huerta R 2013 On the performance of gas sensor arrays in open sampling systems using inhibitory support vector machines *Sens. Actuators B* **185** 462–77

[35] Ackels T, Erskine A, Dasgupta D, Marin A C, Warner T P, Tootoonian S, Fukunaga I, Harris J J and Schaefer A T 2021 Fast odour dynamics are encoded in the olfactory system and guide behaviour *Nature* **593** 558–63

[36] Dennler N, Drix D, Warner T P, Rastogi S, Casa C D, Ackels T, Schaefer A T, van Schaik A and Schmuker M 2024 High-speed odor sensing using miniaturized electronic nose *Sci. Adv.* **10** ead1764

[37] Fackrell J E and Robins A G 1982 The effects of source size on concentration fluctuations in plumes *Bound.-Layer Meteorol.* **22** 335–50

[38] Hopfield J J 1991 Olfactory computation and object perception *Proc. Natl Acad. Sci.* **88** 6462–6

[39] Weissburg M J, Dusenbery D B, Ishida H, Janata J, Roberts P J W and Webster D R 2002 A Multidisciplinary study of spatial and temporal scales containing information in turbulent chemical plume tracking *Environ. Fluid Mech.* **2** 65–94

[40] Moore P and Crimaldi J 2004 Odor landscapes and animal behavior: tracking odor plumes in different physical worlds *J. Mar. Syst.* **49** 55–64

[41] Riffell J A, Shlizerman E, Sanders E, Abrell L, Medina B, Hinterwirth A J and Kutz J N 2014 Flower discrimination by pollinators in a dynamic chemical environment *Science* **344** 1515–8

[42] Schmuker M, Bahr V and Huerta R 2016 Exploiting plume structure to decode gas source distance using metal-oxide gas sensors *Sens. Actuators B* **235** 636–46

[43] Yee E, Chan R, Kosteniuk P R, Chandler G M, Biltoft C A and Bowers J F 1995 The vertical structure of concentration fluctuation statistics in plumes dispersing in the atmospheric surface layer *Bound.-Layer Meteorol.* **76** 41–67

[44] Szyszka P, Gerkin R C, Galizia C G and Smith B H 2014 High-speed odor transduction and pulse tracking by insect olfactory receptor neurons *Proc. Natl Acad. Sci.* **111** 16925–30

[45] Egea-Weiss A, Renner A, Kleineidam C J and Szyszka P 2018 High precision of spike timing across olfactory receptor neurons allows rapid odor coding in *Drosophila iScience* **4** 76–83

[46] Crimaldi J, Lei H, Schaefer A, Schmuker M, Smith B H, True A C, Verhagen J V and Victor J D 2022 Active sensing in a dynamic olfactory world *J. Comput. Neurosci.* **50** 1–6

[47] van Breugel F and Dickinson M 2014 Plume-tracking behavior of flying *Drosophila* emerges from a set of distinct sensory-motor reflexes *Curr. Biol.* **24** 274–86

[48] Szyszka P, Emonet T and Edwards T L 2023 Extracting spatial information from temporal odor patterns: insights from insects *Curr. Opin. Insect Sci.* **59** 101082

[49] Lipinski C A, Lombardo F, Dominy B W and Feeney P J 1996 Experimental and computational approaches to estimate solubility and permeability in drug discovery and development settings *Adv. Drug. Deliv. Rev.* **23** 3–25

[50] Reymond J 2015 The chemical space project *Acc. Chem. Res.* **48** 722–30

[51] Ruddigkeit L, Van Deursen R, Blum L C and Reymond J 2012 Enumeration of 166 billion organic small molecules in the chemical universe database GDB-17 *J. Chem. Inf. Model.* **52** 2864–75

[52] Mayhew E J, Arayata C J, Gerkin R C, Lee B K, Magill J M, Snyder L L, Little K A, Yu C W and Mainland J D 2022 Transport features predict if a molecule is odorous *Proc. Natl Acad. Sci.* **119** e2116576119

[53] Vosshall L B 2000 Olfaction in *Drosophila Curr. Opin. Neurobiol.* **10** 498–503

[54] Paoli M and Galizia G C 2021 Olfactory coding in honeybees *Cell Tissue Res.* **383** 35–58

[55] Kenneth S S 2020 *Anatomy & Physiology: The Unity of Form and Function* (McGraw Hill)

[56] Dunkel A, Steinhaus M, Kotthoff M, Nowak B, Krautwurst D, Schieberle P and Hofmann T 2014 Nature's chemical signatures in human olfaction: a foodborne perspective for future biotechnology *Angew. Chem., Int. Ed.* **53** 7124–43

[57] Photopoulos J 2022 The dogs learning to sniff out disease *Nature* **606** S10–S11

[58] Malnic B, Hirono J, Sato T and Buck L B 1999 Combinatorial receptor codes for odors *Cell* **96** 713–23

[59] De Bruyne M, Foster K and Carlson J R 2001 Odor coding in the *Drosophila* antenna *Neuron* **30** 537–52

[60] Kajiya K, Inaki K, Tanaka M, Haga T, Kataoka H and Touhara K 2001 Molecular bases of odor discrimination: reconstitution of olfactory receptors that recognize overlapping sets of odorants *J. Neurosci.* **21** 6018–25

[61] Hallem E A and Carlson J R 2006 Coding of odors by a receptor repertoire *Cell* **125** 143–60

[62] Pelz D, Roeske T, Syed Z, Bruyne M D and Galizia C G 2006 The molecular receptive range of an olfactory receptor *in vivo* (*Drosophila melanogaster* Or22a) *J. Neurobiol.* **66** 1544–63

[63] Ma L, Qiu Q, Gradwohl S, Scott A, Yu E Q, Alexander R, Wiegraebe W and Yu C R 2012 Distributed representation of chemical features and tunotopic organization of glomeruli in the mouse olfactory bulb *Proc. Natl Acad. Sci.* **109** 5481–6

[64] Münch D and Galizia C G 2016 DoOR 2.0—comprehensive mapping of *Drosophila melanogaster* odorant responses *Sci. Rep.* **6** 21841

[65] Wachowiak M, Dewan A, Bozza T, O'Connell T F and Hong E J 2025 Recalibrating olfactory neuroscience to the range of naturally occurring odor concentrations *J. Neurosci.* **45** e1872242024

[66] Zhang D, Li Y, Wu S and Rasch M J 2013 Design principles of the sparse coding network and the role of "sister cells" in the olfactory system of Drosophila *Front. Comput. Neurosci.* **7** 141

[67] Burton S D, Brown A, Eiting T P, Youngstrom I A, Rust T C, Schmuker M and Wachowiak M 2022 Mapping odorant sensitivities reveals a sparse but structured representation of olfactory chemical space by sensory input to the mouse olfactory bulb *eLife* **11** e80470

[68] Conway M, Oncul M, Allen K, Zhang Z and Johnston J 2024 Perceptual constancy for an odor is acquired through changes in primary sensory neurons *Sci. Adv.* **10** eado9205

[69] Ito I, Ong R C, Raman B and Stopfer M 2008 Sparse odor representation and olfactory learning *Nat. Neurosci.* **11** 1177–84

[70] Papadopoulou M, Cassenaer S, Nowotny T and Laurent G 2011 Normalization for sparse encoding of odors by a wide-field interneuron *Science* **332** 721–5

[71] Rinberg D, Koulakov A and Gelperin A 2006 Sparse odor coding in awake behaving mice *J. Neurosci.* **26** 8857–65

[72] Koulakov A and Rinberg D 2011 Sparse incomplete representations: a potential role of olfactory granule cells *Neuron* **72** 124–36

[73] Persaud K and Dodd G 1982 Analysis of discrimination mechanisms in the mammalian olfactory system using a model nose *Nature* **299** 352–5

[74] Wang C *et al* 2024 Biomimetic olfactory chips based on large-scale monolithically integrated nanotube sensor arrays *Nat. Electron.* **7** 157–67

[75] Laplatine L, Fournier M, Gaignebet N, Hou Y, Mathey R, Herrier C, Liu J, Descloux D, Gautheron B and Livache T 2022 Silicon photonic olfactory sensor based on an array of 64 biofunctionalized Mach-Zehnder interferometers *Opt. Express* **30** 33955

[76] Weber I C, Rüedi P, Šot P, Güntner A T and Pratsinis S E 2022 Handheld device for selective benzene sensing over toluene and xylene *Adv. Sci.* **9** 2103853

[77] van den Broek J, Abegg S, Pratsinis S E and Güntner A T 2019 Highly selective detection of methanol over ethanol by a handheld gas sensor *Nat. Commun.* **10** 4220

[78] Kandel E R *et al* 2000 *Principles of Neural Science* vol 4 (McGraw-Hill)

[79] Buck L and Axel R 1991 A novel multigene family may encode odorant receptors: a molecular basis for odor recognition *Cell* **65** 175–87

[80] Pearce T, Fulvi-Mari C, Covington J, Tan F, Gardner J, Koickal T and Hamilton A 2005 Silicon-based neuromorphic implementation of the olfactory pathway *Conf. Proc. 2nd Int. IEEE EMBS Conf. on Neural Engineering, 2005* (IEEE) pp 307–12

[81] Koickal T, Hamilton A, Pearce T, Tan S, Covington J and Gardner J 2006 Analog VLSI design of an adaptive neuromorphic chip for olfactory systems *2006 IEEE Int. Symp. on Circuits and Systems* (IEEE) pp 4547–50

[82] Koickal T J, Hamilton A, Tan S L, Covington J A, Gardner J W and Pearce T C 2007 Analog VLSI circuit implementation of an adaptive neuromorphic olfaction chip *IEEE Trans. Circuits Syst. I* **54** 60–73

[83] Hsieh H-Y and Tang K-T 2012 VLSI implementation of a bio-inspired olfactory spiking neural network *IEEE Trans. Neural Netw. Learn. Syst.* **23** 1065–73

[84] Schmuker M, Pfeil T and Nawrot M P 2014 A neuromorphic network for generic multivariate data classification *Proc. Natl Acad. Sci.* **111** 2081–6

[85] Diamond A, Schmuker M, Berna A Z, Trowell S and Nowotny T 2016 Classifying continuous, real-time e-nose sensor data using a bio-inspired spiking network modelled on the insect olfactory system *Bioinspir. Biomim.* **11** 026002

[86] Jing Y, Meng Q, Qi P, Zeng M and Liu Y 2017 Signal processing inspired from the olfactory bulb for electronic noses *Meas. Sci. Technol.* **28** 015105

[87] Han J, Kang M, Jeong J, Cho I, Yu J, Yoon K, Park I and Choi Y 2022 Artificial olfactory neuron for an in-sensor neuromorphic nose *Adv. Sci.* **9** 2106017

[88] Wang T, Wang X, Wen J, Shao Z, Huang H and Guo X 2022 A bio-inspired neuromorphic sensory system *Adv. Intell. Syst.* **4** 2200047

[89] Stasenko S V, Mikhaylov A N and Kazantsev V B 2023 Model of neuromorphic odorant-recognition network *Biomimetics* **8** 277

[90] Pearce T, Verschure P, White J and Kauer J 2001 Robust stimulus encoding in olfactory processing: hyperacuity and efficient signal transmission *Emergent Neural Computational Architectures Based on Neuroscience: Towards Neuroscience-Inspired Computing* (Springer) pp 461–79

[91] Jürgensen A, Khalili A, Chicca E, Indiveri G and Nawrot M P 2021 A neuromorphic model of olfactory processing and sparse coding in the Drosophila larva brain *Neuromorph. Comput. Eng.* **1** 024008

[92] Guo W, Fouda M E, Eltawil A M and Salama K N 2021 Neural coding in spiking neural networks: a comparative study for robust neuromorphic systems *Front. Neurosci.* **15** 638474

[93] Ng K T, Guo B, Bermak A, Martinez D and Boussaid F 2009 Characterization of a logarithmic spike timing encoding scheme for a 4×4 tin oxide gas sensor array *2009 IEEE Sensors* (IEEE) pp 731–4

[94] Ng K T, Boussaid F and Bermak A 2011 A CMOS single-chip gas recognition circuit for metal oxide gas sensor arrays *IEEE Trans. Circuits Syst. I* **58** 1569–80

[95] Chen H T, Ng K T, Bermak A, Law M K and Martinez D 2011 Spike latency coding in biologically inspired microelectronic nose *IEEE Trans. Biomed. Circuits Syst.* **5** 160–8

[96] Yamani J A, Boussaid F, Bermak A and Martinez D 2012 Glomerular latency coding in artificial olfaction *Front. Neuroeng.* **4** 18

[97] Hassan M, Bermak A, Ali A A S and Amira A 2015 Gas identification with spike codes in wireless electronic nose: a potential application for smart green buildings *2015 SAI Intelligent Systems Conf. (IntelliSys)* (IEEE) pp 457–62

[98] Huo D, Zhang J, Dai X, Zhang P, Zhang S, Yang X, Wang J, Liu M, Sun X and Chen H 2023 A bio-inspired spiking neural network with few-shot class-incremental learning for gas recognition *Sensors* **23** 2433

[99] Vanarse A, Espinosa-Ramos J I, Osseiran A, Rassau A and Kasabov N 2020 Application of a brain-inspired spiking neural network architecture to odor data classification *Sensors* **20** 2756

[100] Yan J, Wu B, Liu T, Chen F and Dua S 2023 An SNN-based bionic olfactory signal processing network for odor recognition *IEEE Sens. J.* **23** 13186–97

[101] Pearce T C, Karout S, Rácz Z, Capurro A, Gardner J W and Cole M 2013 Rapid processing of chemosensor transients in a neuromorphic implementation of the insect macroglomerular complex *Front. Neurosci.* **7** 119

[102] Vanarse A, Osseiran A, Rassau A and Van Der Made P 2019 A hardware-deployable neuromorphic solution for encoding and classification of electronic nose data *Sensors* **19** 4831

[103] Dennler N, Drix D, Rastogi S, Schaik A V and Schmuker M 2022 Rapid inference of geographical location with an event-based electronic nose *9th Annual Neuro-Inspired Computational Elements (NICE)* vol 1 (Association for Computing Machinery)

[104] Vanarse A, Osseiran A, Rassau A and Van Der Made P 2022 Application of neuromorphic olfactory approach for high-accuracy classification of malts *Sensors* **22** 440

[105] Barsan N and Weimar U 2001 Conduction model of metal oxide gas sensors *J. Electroceram.* **7** 143–67

[106] Fukunaga I, Berning M, Kollo M, Schmaltz A and Schaefer A T 2012 Two distinct channels of olfactory bulb output *Neuron* **75** 320–9

[107] Rastogi S, Dennler N, Schmuker M and Van Schaik A 2023 Spike-time encoding of gas concentrations using neuromorphic analog sensory front-end *2023 IEEE Biomedical Circuits and Systems Conf. (BioCAS)* (IEEE) pp 1–5

[108] Rastogi S, Dennler N, Schmuker M and Schaik A V 2024 The neuromorphic analog electronic nose (arXiv:2410.16677 [cs])

[109] Rastogi S, Dennler N, Schmuker M and Schaik A V 2024 Neuromorphic circuit for temporal odor encoding in turbulent environments (arXiv:2412.20117 [cs])

[110] Gütig R and Sompolinsky H 2009 Time-warp–invariant neuronal processing *PLoS Biol.* **7** e1000141

[111] Lewis S M, Suarez L M, Rigolli N, Steinmetz N A and Gire D H 2024 The spiking output of the mouse olfactory bulb encodes large-scale temporal features of natural odor environments *bioRxiv Preprint* (Accessed 1 April 2025) (https://doi.org/10.1101/2024.03.01.582978)

[112] Park I J, Hein A M, Bobkov Y V, Reidenbach M A, Ache B W and Principe J C 2016 Neurally encoding time for olfactory navigation *PLoS Comput. Biol.* **12** e1004682

[113] Kadakia N, Demir M, Michaelis B T, DeAngelis B D, Reidenbach M A, Clark D A and Emonet T 2022 Odour motion sensing enhances navigation of complex plumes *Nature* **611** 754–61

[114] Rigolli N, Magnoli N, Rosasco L and Seminara A 2022 Learning to predict target location with turbulent odor plumes *eLife* **11** e72196

[115] Drix D and Schmuker M 2021 Resolving fast gas transients with metal oxide sensors *ACS Sens.* **6** 688–92

[116] Martinez D, Burgués J and Marco S 2019 Fast measurements with MOX sensors: a least-squares approach to blind deconvolution *Sensors* **19** 4029

[117] Maass W 1997 Networks of spiking neurons: the third generation of neural network models *Neural Netw.* **10** 1659–71

[118] Raman B, Sun P A, Gutierrez-Galvez A and Gutierrez-Osuna R 2006 Processing of chemical sensor arrays with a biologically inspired model of olfactory coding *IEEE Trans. Neural Netw.* **17** 1015–24

[119] Borthakur A and Cleland T A 2019 A spike time-dependent online learning algorithm derived from biological olfaction *Front. Neurosci.* **13** 656

[120] Imam N and Cleland T A 2020 Rapid online learning and robust recall in a neuromorphic olfactory circuit *Nat. Mach. Intell.* **2** 181–91

[121] Dennler N, van Schaik A and Schmuker M 2024 Limitations in odour recognition and generalization in a neuromorphic olfactory circuit *Nat. Mach. Intell.* **6** 1451–3

[122] Dai X, Huo D, Gao Z, Zhang J and Chen H 2023 A visual-olfactory multisensory fusion spike neural network for early fire/smoke detection *Research Square Preprint* (Accessed 1 April 2025) (https://doi.org/10.21203/rs.3.rs-3192562/v1)

[123] Dalgaty T, Vianello E, De Salvo B and Casas J 2018 Insect-inspired neuromorphic computing *Curr. Opin. Insect Sci.* **30** 59–66

[124] Beyeler M, Stefanini F, Proske H, Galizia G and Chicca E 2010 Exploring olfactory sensory networks: simulations and hardware emulation *2010 Biomedical Circuits and Systems Conf. (BioCAS)* (IEEE) pp 270–3

[125] Pfeil T, Grübl A, Jeltsch S, Müller E, Müller P, Petrovici M A, Schmuker M, Brüderle D, Schemmel J and Meier K 2013 Six networks on a universal neuromorphic computing substrate *Front. Neurosci.* **7** 11

[126] Arena P, Patané L and Termini P S 2012 Learning expectation in insects: a recurrent spiking neural model for spatio-temporal representation *Neural Netw.* **32** 35–45

[127] Arena P, Cali M, Patane L, Portera A and Strauss R 2015 A mushroom bodies inspired spiking network for classification and sequence learning *2015 Int. Joint Conf. on Neural Networks (IJCNN)* (IEEE) pp 1–8

[128] Hausler C, Nawrot M P and Schmuker M 2011 A spiking neuron classifier network with a deep architecture inspired by the olfactory system of the honeybee *2011 5th Int. IEEE/EMBS Conf. on Neural Engineering* (IEEE) pp 198–202

[129] Rapp H and Nawrot M P 2020 A spiking neural program for sensorimotor control during foraging in flying insects *Proc. Natl Acad. Sci.* **117** 28412–21

[130] Arena P, Li Noce A, Patane L and Taffara S 2022 Insect-inspired spiking neural controllers for adaptive behaviors in bio-robots *IEEE Instrum. Meas. Mag.* **25** 19–27

[131] Jesusanmi O O, Amin A A, Domcsek N, Knight J C, Philippides A, Nowotny T and Graham P 2024 Investigating visual navigation using spiking neural network models of the insect mushroom bodies *Front. Physiol.* **15** 1379977

[132] Milde M B *et al* 2022 Neuromorphic engineering needs closed-loop benchmarks *Front. Neurosci.* **16** 813555

[133] Tanaka G, Yamane T, Héroux J B, Nakane R, Kanazawa N, Takeda S, Numata H, Nakano D and Hirose A 2019 Recent advances in physical reservoir computing: a review *Neural Netw.* **115** 100–23

[134] Modi M N, Shuai Y and Turner G C 2020 The *Drosophila* mushroom body: from architecture to algorithm in a learning circuit *Annu. Rev. Neurosci.* **43** 465–84

[135] Kasabov N *et al* 2016 Evolving spatio-temporal data machines based on the NeuCube neuromorphic framework: design methodology and selected applications *Neural Netw.* **78** 1–14

[136] Wang T, Huang H, Wang X and Guo X 2021 An artificial olfactory inference system based on memristive devices *InfoMat* **3** 804–13

[137] Abdi G, Alluhaibi L, Kowalewska E, Mazur T, Mech K, Podborska A, Sławek A, Tanaka H and Szaciłowski K 2023 Reservoir computing and photoelectrochemical sensors: a marriage of convenience *Coord. Chem. Rev.* **487** 215155

[138] Lilienthal A J, Loutfi A and Duckett T 2006 Airborne chemical sensing with mobile robots *Sensors* **6** 1616–78

[139] Kowadlo G and Russell R A 2008 Robot odor localization: a taxonomy and survey *Int. J. Robot. Res.* **27** 869–94

[140] Francis A, Li S, Griffiths C and Sienz J 2022 Gas source localization and mapping with mobile robots: a review *J. Field Robot.* **39** 1341–73

[141] Wang L, Pang S, Noyela M, Adkins K, Sun L and El-Sayed M 2023 Vision and olfactory-based wildfire monitoring with uncrewed aircraft systems *2023 20th Int. Conf. on Ubiquitous Robots (UR)* (IEEE) pp 716–23

[142] Duisterhof B P, Li S, Burgues J, Reddi V J and De Croon G C H E 2021 Sniffy bug: a fully autonomous swarm of gas-seeking nano quadcopters in cluttered environments *2021 IEEE/RSJ Int. Conf. on Intelligent Robots and Systems (IROS)* (IEEE) pp 9099–106

[143] Fan H, Hernandez Bennetts V, Schaffernicht E and Lilienthal A 2019 Towards gas discrimination and mapping in emergency response scenarios using a mobile robot with an electronic nose *Sensors* **19** 685